Bubble generation in swirl flow during air-sparged hydrocyclone flotation

D. Lelinski, R. Bokotko, J. Hupka and J.D. Miller

Abstract — *Air-sparged hydrocyclone (ASH) flotation is a new, promising technology, and, since its conception, numerous applications have been successfully tested. Nevertheless, research and development efforts have continued to improve the technology with respect to operating conditions and design considerations.*

Results from experimental studies on bubble generation in the ASH system are presented in this paper. Bubble size distributions generated during ASH operation were determined using a high-speed photographic technique. The influence of many factors, including surfactant concentration, water flow rate, and porous-tube pore size have been studied. Test results indicate that these process variables have a profound effect on the bubble size distribution. With an increase in surfactant concentration or water flow rate (shear field), the bubble size distributions become narrower and shift toward smaller average bubble diameters. However, the influence of pore size is more complicated. Depending on the experimental conditions, the average bubble size was found to range from about 100 to 300 μm in diameter.

Introduction

The air-sparged hydrocyclone is distinguished by its high capacity for fine-particle flotation in a centrifugal field. For example, it is now evident that the ASH has a specific capacity of at least 100 times that of conventional flotation equipment. During the 1980s, small 2-in.-diam ASH units were tested for a large number of mineral commodities, and design modifications were made as necessary (Miller and Ye, 1989). The air-sparged hydrocyclone has shown promise for the flotation of copper porphyry ore, low-grade placer gold and auriferous pyrite ores, iron ore, phosphate rock, potash, various other industrial minerals and fine-coal cleaning. In addition, the effectiveness of the ASH system has been successfully demonstrated for various environmental applications such as oil and VOC removal from wastewater and deinking flotation for wastepaper recycle. Development efforts have also been extended to other countries, including Australia, Brazil, Canada, Chile, Israel, Mexico, Netherlands, Poland and South Africa.

Bubble size is always of interest in the analysis of flotation separations. Many researchers believe that bubble size is a critical factor that controls the rate of flotation and the efficiency of separation. During ASH flotation, air is sparged through the porous tube wall and is sheared into numerous small bubbles by the high velocity swirl flow of the slurry. In this regard, measurement of the size of the bubbles during ASH flotation is rather difficult. Several theoretical approaches (Miller and Kinneberg, 1984; Miller et al., 1985; Miller and Ye, 1989) have been used to estimate the average bubble size. Also high-speed video measurements of bubble size for bubble production from a single capillary have been reported for a model swirl-flow system (Miller and Ye, 1989). It was found that the bubble size was comparable to the capillary diameter and increased with an increase in the air flow rate. These results were in general agreement with theory. Surprisingly, it was found in this model swirl-flow system that the surface tension did not influence the bubble size generated from a single capillary. However, later studies (Miller et al., 1993a, 1993b; Hupka, 1994) indicated that surface tension is, in fact, a critical variable in establishing bubble size distribution under actual ASH flotation conditions. These studies (Miller et al., 1993a, 1993b; Hupka et al., 1994) have also examined the dependence of bubble size on other process variables, such as ASH diameter, ASH length and dimensionless flow-rate ratio.

A main drawback of these past studies was that the photographic equipment employed could only capture bubbles that were coarser than 300 μm. To rectify this situation, studies were undertaken with new photographic equipment with which bubbles finer than 20 μm can be measured at speeds of 1 m/sec. Results of these studies are presented in this paper.

Experimental

Among a number of different techniques that have been developed over the years to measure bubble size in liquids, a photographic technique was selected and adapted for this research. A conventional 35-mm camera (Pentax K1000)

D. Lelinski, member SME, is graduate student with the University of Utah, Salt Lake City, UT; **R. Bokotko** and **J. Hupka** are with the Technical University of Gdansk, Gdansk, Poland; and **J.D. Miller**, member SME, is professor with the University of Utah, Salt Lake City, UT. SME preprint 95-173, SME Annual Meeting, March 6-9, 1995, Denver, CO. Original manuscript, February 1995. M&MP paper 95-618. Discussion of this peer-reviewed and approved paper is invited and must be submitted, in duplicate, prior to Aug. 31, 1996.

Table 1 — Average bubble diameters calculated from size distributions for different ASH operating conditions.

Porous Tube size	SDS Concentration, M	Average diameter, μm			Sauter diameter, μm		
		Inlet water pressure, psi					
		2.5	5.0	10.0	2.5	5.0	10.0
Fine	$1x10^{-6}$	1028	891	755	1785	1367	1178
	$1x10^{-5}$	792	703	486	1591	1231	945
	$5x10^{-5}$	583	496	309	1340	985	786
	$1x10^{-4}$	449	409	249	1201	857	708
	$5x10^{-4}$	369	257	176	967	666	478
	$1x10^{-3}$	286	219	149	787	579	411
Medium	$1x10^{-6}$	968	747	674	2267	1664	1306
	$1x10^{-5}$	716	597	428	2098	1436	1135
	$5x10^{-5}$	528	412	339	1953	1268	1025
	$1x10^{-4}$	491	392	305	1790	1178	896
	$5x10^{-4}$	410	275	224	1511	918	726
	$1x10^{-3}$	279	179	161	1359	798	659
Course	$1x10^{-6}$	838	673	539	2532	1798	1491
	$1x10^{-5}$	706	534	376	2322	1685	1359
	$5x10^{-5}$	560	398	279	2122	1469	1191
	$1x10^{-4}$	491	333	236	2009	1286	1086
	$5x10^{-4}$	417	231	179	1686	1038	928
	$1x10^{-3}$	358	202	163	1586	923	840

with macro lenses (Pentax A 200 mm F4ED) and an electronic microflash (EG&G model 549-11 type LP-3FB) were used to capture the flow of dispersed bubbles in water moving at a velocity of about 1 m/sec. The preferred measurement location for the determination of the bubble size distribution is inside ASH. However, because of difficulties with lighting and accessibility, it was impossible to carry out such measurements, even in a specially designed and constructed ASH with transparent windows. In this regard, measurements were carried out in the underflow stream during water-only operation of actual ASH units. A 5-cm-diam, 47-cm-long (two sections: 16 and 31 cm) ASH unit (the ASH-2C) with separate, adjustable air supply to both sections was used in all experiments. The froth pedestal of the ASH was replaced by a 90° painted steel cone to improve resolution of the bubbles. The photographs of the underflow stream were taken just as the water discharged from the ASH. The effect of pore size was studied by using porous tubes of the following three pore sizes: fine (20 to 40 μm), medium (40 to 60 μm) and coarse ((70 to 90 μm). The effect of shear force was examined at water flow rates of 35, 52.5 and 70 L/min (2.5, 5.0 and 10.0 psi), and the air flow rate was held constant at 70 L/min for all experiments (divided proportionally between the two ASH sections 23 and 47 L/min). The effect of a surface-active agent — sodium dodecyl sulfate (SDS) — was studied at concentrations from 0 to 10^{-3} M (i.e., 0, 1 x 10^{-5}, 5 x 10^{-5}, 1 x 10^{-4}, 5 x 10^{-4} and 1 x 10^{-3} M).

In most of the literature examined, a major emphasis was placed on the necessity of counting a large number of bubbles to get a meaningful size distribution. Actually, however, statistically significant counts can be made with as few as 300 bubbles. It can be shown (Dixon and Massey, 1957) that a count of 300 bubbles will result in a distribution in which the error for any particular size will be less than 8% with a 95% confidence limit. Reduction of this expected error to 5%, at the same level of confidence, would require the counting of 2,960 bubbles. In view of the other sources of error affecting such measurements, such a small reduction in error hardly seems worth the tenfold increase in effort. As a consequence, 300 bubbles, or more, were measured for each size distribution.

For discussion of bubble size-distribution data, it is useful to consider the average size of each distribution. In this study, the following two different average values were used

$$\bar{d} = \frac{\Sigma d_i n_i}{\Sigma n_i} \qquad (1)$$

$$\bar{d}_{32} = \frac{\Sigma d_i^3 n_i}{\Sigma d_i^2 n_i} \qquad (2)$$

Equation (1) provides a simple arithmetic mean by number, while Eq. (2) yields mean volume-surface diameter (often called the Sauter diameter).

Results and discussion

All average diameters were calculated from measured bubble size distributions and are presented in Table 1.

Surfactant concentration. Typical air-bubble size distributions for different surfactant concentrations are presented in Fig. 1. When the surfactant concentration increases, the size distribution becomes narrower and shifts towards smaller average bubble diameters. These results appear to be due to a decrease in surface tension and confirm earlier predictions for bubble generation from a porous wall under significant shear (Miller and Ye, 1989; Yoon et al., 1989). In Fig. 2 the surface tension results of water used for

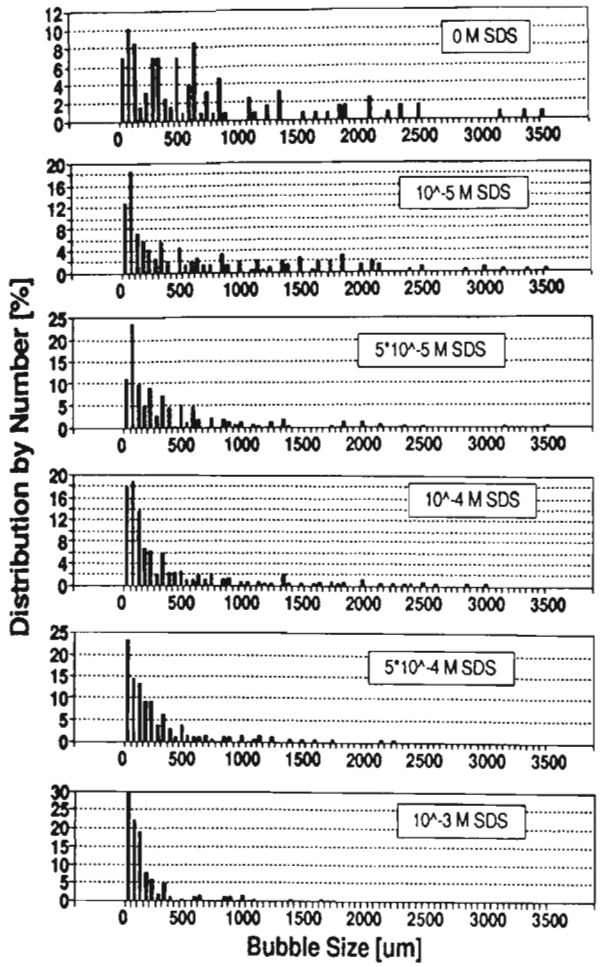

Fig. 1 — Bubble size distribution for different surfactant (SDS) concentrations. Medium pore size, 5.0 psi inlet water pressure.

bubble size measurements is presented as a function of SDS (commercial grade) concentration. These surface tension results with tap water differ significantly from the results with deionized (DI) water (typical of values reported in the literature), as shown in Fig. 2. All ash experiments were performed in the pilot plant (70 L/min) using tap water and commercial-grade surfactant. In the absence of surfactant, the distribution shows a contribution from both large and small bubbles. Large bubbles inside the ASH system are probably due to the coalescence of bubbles generated from adjacent pores. On the other hand, fine bubbles are those nascent bubbles that are not subjected to the above coalescence. In addition, the coalescence of two or more bubbles can also result in the formation of some fine bubbles. Such fine bubbles are sometimes termed satellite bubbles, due to their close proximity to coarser bubbles.

The concentration of surfactant had the most pronounced effect on the average bubble size as calculated from each size distribution (Fig. 3). The simple number average bubble size dropped by almost 75%, but the surface volume average dropped only by 50% with an increase in surfactant concentration of from 0 to 10^{-3} M. Such a change in the bubble size was not observed during the single capillary study (Miller and Ye, 1989). In this regard, it may be concluded that the major role of the surfactant is to prevent coalescence of bubbles as they form at adjacent pores on the porous tube wall (Zieminski et al., 1967; Prakash and Briens, 1990).

Also, it was observed that, with an increase in surfactant concentration, the bubble concentration in the underflow

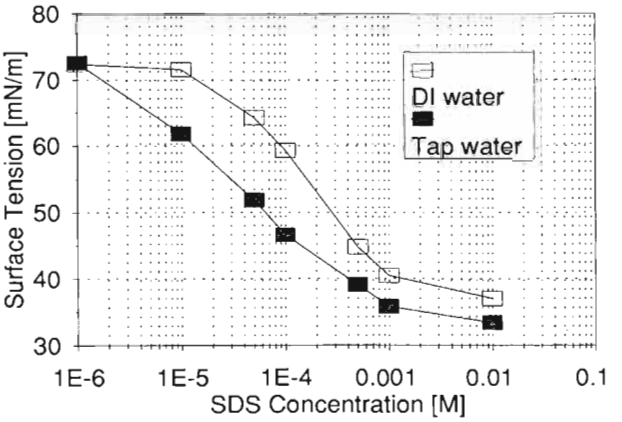

Fig. 2 — Surface tension of commercial grade SDS solutions at natural pH and ambient temperature.

increased, which would be expected due to the smaller bubble size. This observation supports the theoretical analysis by Miller (1995) and Das (1996) that predicted that such transport to the underflow was dependent on the flow characteristics, the bubble size and the location on the porous tube where the bubbles were generated.

Shear force. Bubbles generated during ASH flotation are small because air is sparged through the porous wall and sheared by the high-velocity swirl flow of the slurry. The shear force is proportional to the water-inlet pressure. The change in the magnitude of shear force has a visible influence on bubble size, as is evident from the data presented in Fig. 4 — two examples of variation of bubble size distribution at different inlet pressures with other parameters being kept constant. As in the case of surfactant addition, when the inlet water pressure increases, the bubbles become smaller, and the size distributions become narrower. Both the number average and Sauter diameters demonstrate a similar response to changes in inlet pressure (except at 2.5 psi, see Fig. 3). At this pressure, the Sauter diameter increases rapidly, and this change becomes larger with increases in pore size. Corresponding results have been obtained by other researchers for bubble formation at the surface of a frit under shear flow (Johnson et al., 1982; Johnson and Gershey, 1991).

At higher inlet pressures and higher surfactant concentrations, the bubble size becomes less dependent on shear force. From one perspective, this might be attributed to the fact that, with smaller bubbles, the thickness of the effective hydrodynamic boundary layer for the swirl flow is no longer of any significance. In the absence of surfactant, the bubble size is sufficiently large that the bubble extends beyond the effective boundary layer into the shear flow. In this way, the shear velocity, which, of course, is greater for the higher inlet pressure, leads to small bubbles at higher pressure in the absence of surfactant. On the other hand, in the presence of sufficient surfactant, the bubbles are released at a small size and contained within the boundary layer, due to a reduced surface tension. In addition, the presence of surfactant tends to stabilize these smaller bubbles and prevent coalescence.

Pore size. Two sets of typical bubble size distributions for different porous tube sizes are presented in Fig. 5. The role of pore size in establishing the bubble size distribution is more complex compared to the other process variables examined. Some of the complexity can be explained by comparing calculated number average and Sauter mean diameters (see Fig. 6). As expected, for all conditions, the calculated Sauter

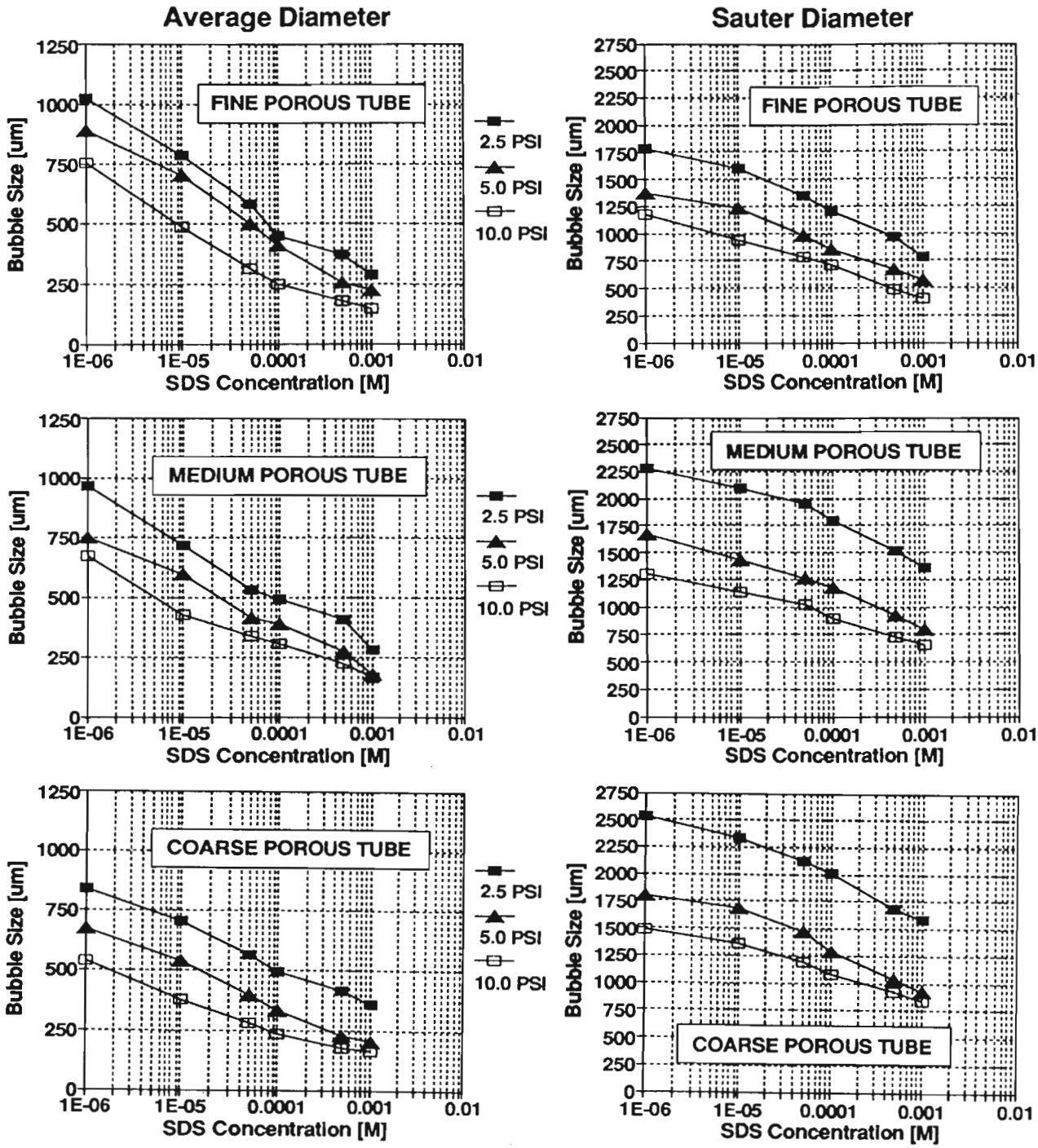

Fig. 3 — Number average and Sauter mean bubble diameters for different pore sizes and operating conditions. Indicated pressure measured at the ASH water inlet.

mean diameter is at a maximum for the coarse pore size and at a minimum at the fine pore size. On the other hand, the number average diameter is largest for fine pore sizes and smallest for the coarse pore size, but this dependence is not as pronounced as in the case of the Sauter mean diameter. For the number average diameter, the variation is most distinct at low concentrations. In general, the presence of a limited number of large bubbles can drastically increase the Sauter diameter. Because the number of such large bubbles increases as pore size increases, it can be expected that coarser pores would generate bubbles with a larger Sauter diameter. On the other hand, at this time, it is not well understood why the average bubble diameter decreases (although only slightly and at high surface tension) with increasing pore size. The following are possible reasons:

- a lower coalescence for the coarse pore size in which the average distance between the adjacent pores is greater than that for the fine porous tube;
- bubble growth protection by higher porosity of coarser porous tube (more extended laminar layer), larger bubbles are later torn apart by a high-shear field; and
- a more predominant role of shear and surface tension than pore size on bubble formation.

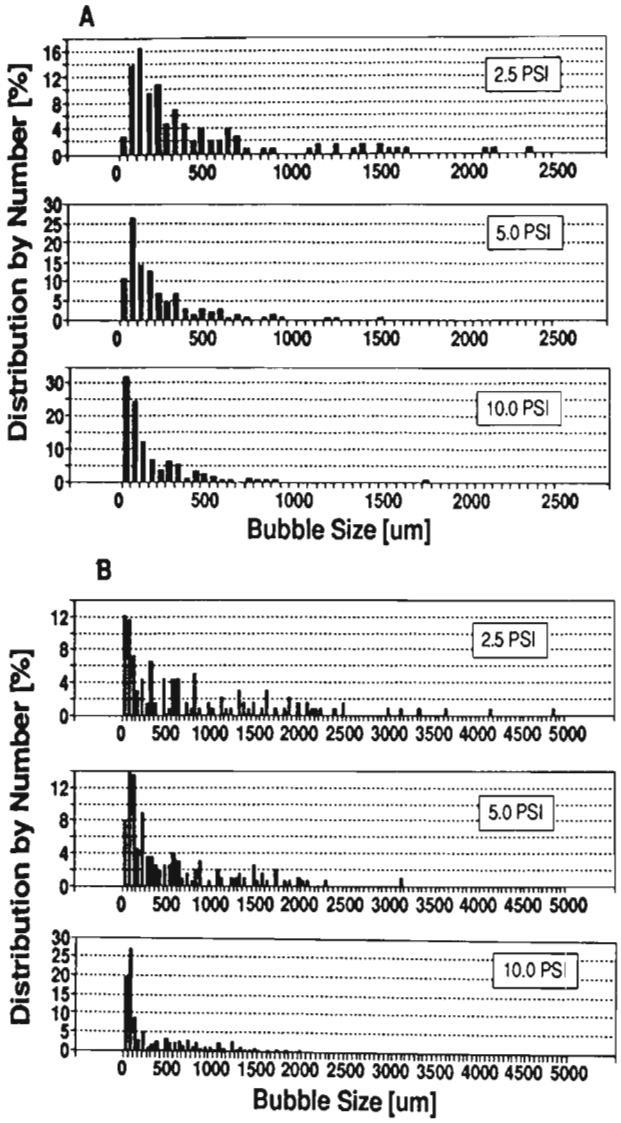

Fig.4 — Bubble size distributions for different inlet water pressures: (A) = fine pore size, 5 x 10^{-4} M SDS; (B) = coarse pore size, 10^{-5} M SDS.

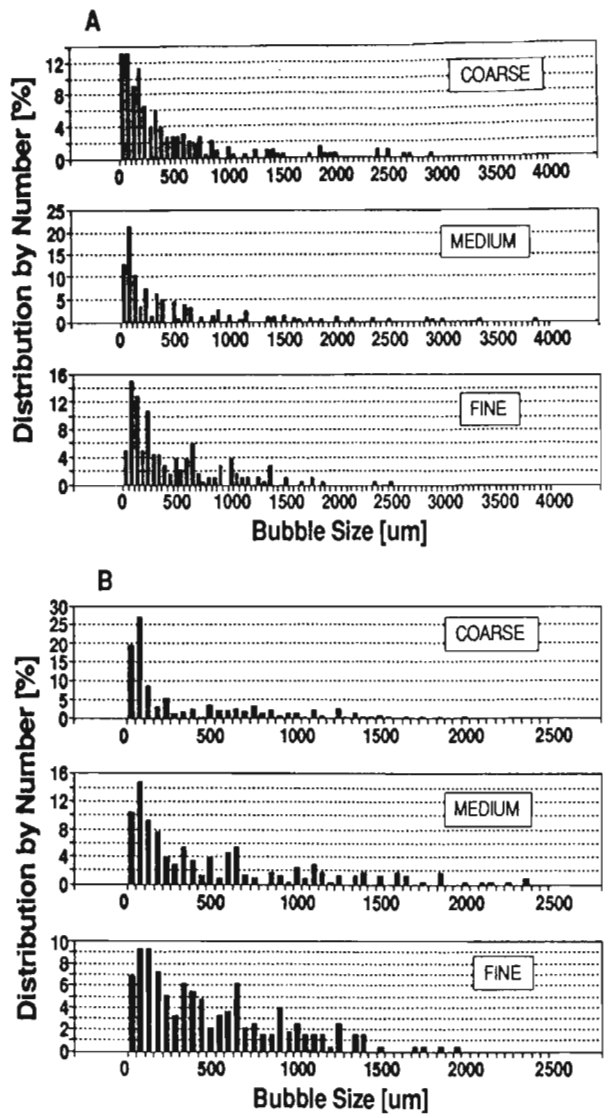

Fig.5 — Bubble size distributions for different pore sizes: (A) = 2.5 psi inlet water pressure, 5 x 10^{-5} M SDS; (B) = 10.0 psi inlet water pressure, 10^{-5} M SDS.

In this regard, it is worth mentioning that, in the case of coal flotation tests with ASH-2C, the efficiency of flotation separations were nearly the same for all pore sizes (Stoessner et al., 1990).

Conclusions

Bubble size distribution in an actual ASH system was measured using photographic equipment that was capable of capturing bubbles smaller than 20 μm moving with linear velocities higher than 1 m/sec. The experimental results were discussed in terms of surfactant stabilization of bubbles formed at individual pores, pore sizes and the effective thickness of the hydrodynamic boundary layer controlled by shear force.

Based on previous research results (Miller et al., 1993a, 1993b; Hupka, 1994), it is believed that the sparged air might create a blanket, or cushion, of air that covers the inside wall of the porous tube and, thus, creates a "frictionless" surface. Evidence for this phenomenon was found from the radial density gradients as determined by X-ray CT measurements (Miller et al., 1993a, 1993b). From this perspective, the blanket of air is sheared or broken into bubbles the size of which might simply be controlled by the size of turbulent eddies. In this case, the pore size of the porous tube would have little effect on the bubble size distribution, but, based on these experimental results, the mechanism of bubble formation in the ASH is more complex. At low surfactant concentration, the change in pore size affects the size of the generated bubbles. After coalescence of the adjacent bubbles, the formed bubbles are larger and extend over the hydrodynamic boundary layer. The mechanism of coalescence and the interaction during bubble separation from the porous wall is influenced by the size of the pore, roughness of the wall surface and distance between pores. The air-cushion mechanism, described earlier, is more probable for higher surfactant concentration, when the bubble diameter is smaller than the hydrodynamic boundary layer.

References

Das, A., and Miller, J.D. 1996, "Swirl flow characteristics and froth phase features in air-sparged hydrocyclone flotation as revealed by X-ray CT analysis," *International Journal of Mineral Processing*, to be published.

Dixon, W.J., and Massey, F.J., Jr., 1957, *Introduction to Statistical Analysis*, 2nd Ed., McGraw-Hill Book Co. Inc., New York, p. 292.

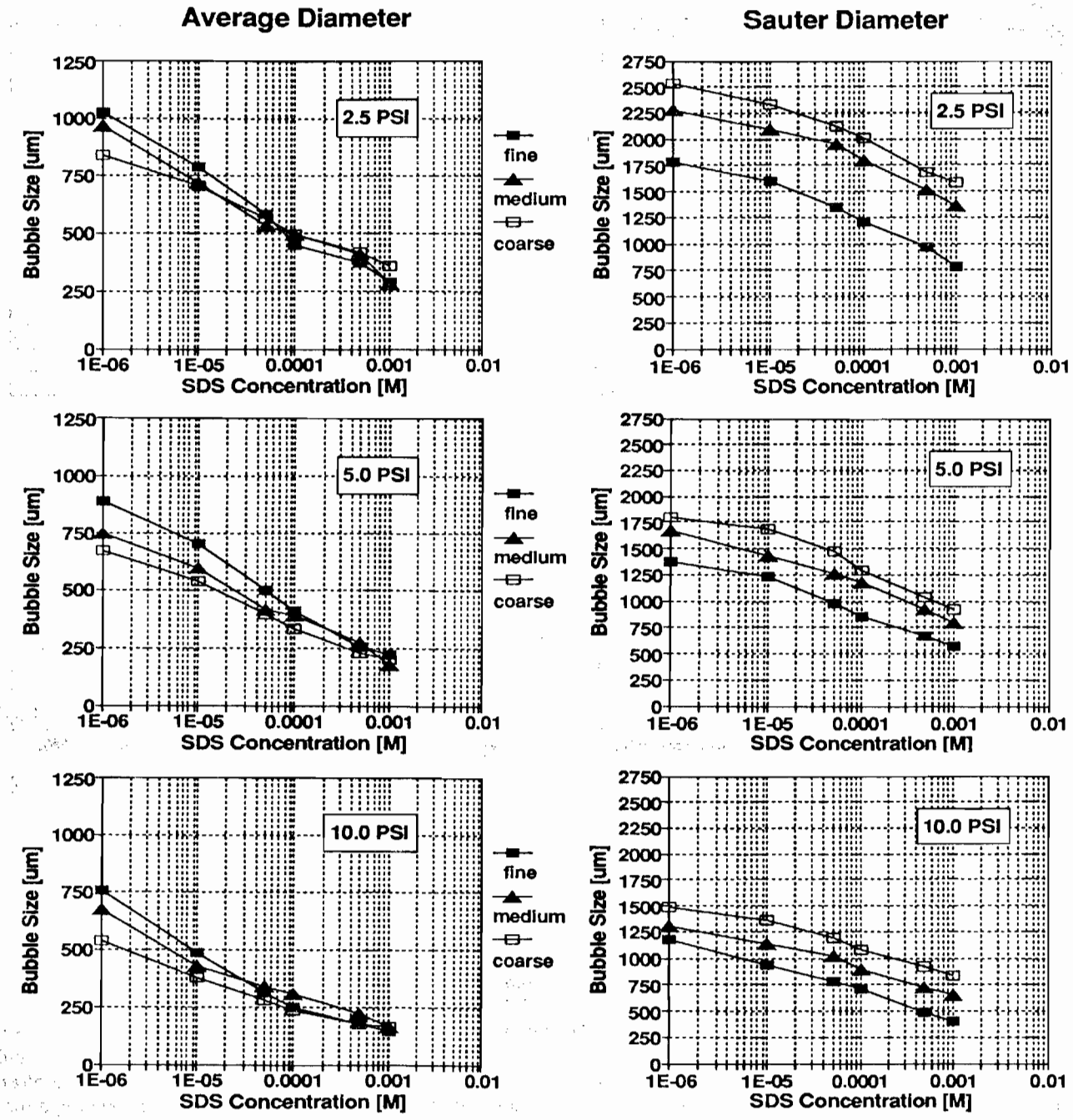

Fig.6 — Number average and Sauter mean bubble diameters for different pore sizes and opperating conditions. Indicated pressure measured at the ASH water inlet.

Hupka, J., Bokotko, R.P., Lelinski, D., and Miller, J.D., 1994, "Bubble size distribution in air-sparged hydrocyclone," *Proceedings of the 12th International Coal Preparation Congress*, Cracow, Poland, May 27, pp. 1267-1273.

Johnson, B.D., Gershey, R.M., Cooke, R.C., and Sutcliffe, W.H., Jr., 1982, "A theoretical model for bubble formation at a frit surface in a shear field," *Separation Science and Technology*, Vol. 17, No. 8, pp. 1027-1039.

Johnson, B.D., and Gershey, R.M., 1991, "Bubble formation at a cylindrical frit surface in a shear field," *Chemical Engineering Science*, Vol. 46, No. 10, pp. 2753-2756.

Miller, J.D., and Kinneberg, D.J., 1984, "Fast flotation in an air-sparged hydrocyclone," *Proceedings of MINTEK 50*, South Africa, Vol. 1, March, pp. 373-383.

Miller, J.D., Upadrashta, K.R, Kinneberg, D.J., and Gopalakrishnan, S., 1985, "Fluid-flow phenomena in the air-sparged hydrocyclone," *Proceedings of the XV International Mineral Processing Congress*, Cannes, July 2-9, pp. 87-99.

Miller, J.D., and Ye, Y., 1989, "Froth characteristics in air-sparged hydrocyclone flotation," *Mineral Processing & Extractive Metallurgy Review*, Vol. 5, pp. 307-329.

Miller, J.D., Das, A., Lelinski, D., and Chamblee, J.W., 1993a, "Multiphase flow characteristics of gas sparged hydrocyclones flotation deinking," *Proceedings of the 1993 TAPPI Engineering conference: Fluid Mechanics of Deinking and Recycling*, Book 2, Orlando, FL, September 20-30, pp. 417-428.

Miller, J.D., Ye, Y., Hupka, J., Das, A., and Lelinski, D., 1993b, "Research and development efforts in air-sparged hydrocyclone flotation for fine coal cleaning," presented at the 122nd SME Annual Meeting, Reno, NV, February 15-18.

Miller, J.D., and Das, A., 1995, Flow phenomena and its impact on air-sparged hydrocyclone flotation on quartz," *Minerals and Metallurgical Processing*, February, pp. 51-63

Prakash, A., and Briens, C.L., 1990, "Porous gas distributors in bubble columns. effect of liquid presence on distributor pressure drop. effect of start-up procedure on distributor performance, " *The Canadian Journal of Chemical Engineering*, Vol. 68, pp. 204-210.

Stoessner, R.D., Shirey, G.A., Zawadski, E.A., Welsh, C.F., Miller, J.D., and Shell, W.P., 1990, "Air-sparged hydrocyclone/advanced froth flotation fine coal cleaning," Final Report, DOE Contract NO. DE-AC22-88PC88853.

Yoon, R. H., Lutterell, G. H., Adel, G. T., and Mankosa, M. J., 1989, "Recent advances in fine coal flotation," *Proceedings of the Engineering Foundation Conference: Advances in coal and mineral processing using flotation*, Palm Coast, FL, December 3-8, pp. 211-218.

Zieminski, S.A., Caron, M.M., and Blackmore, R.B., 1967, "Behavior of air bubble in dilute aqueous solutions," *I&EC Fundamentals*, Vol. 6, No. 2, pp. 233-242.